however, the same problem done with hard-pion techniques did require a cutoff.[21]

One possible physical explanation for the cutoff is given in the vector-dominance model, which says that the strong-interaction vertex (of the vector meson connecting to the hadron line) has an unknown form factor associated with it. Even though the concept of a cutoff (or effective cutoff Λ) is accepted, any derivation of its value from first principles is lacking. The empirical "double-pole" form of the nucleon form factors would suggest an effective cutoff in the range of the vector-meson masses (i.e., 0.7–0.8 BeV) for that case. Since this is smaller than the hadronic mass to which it connects, it has also been suggested that a cutoff in the neighborhood of the hadronic mass is reasonable.

The above discussion would suggest that, for K mesons, a reasonable cutoff would be in the range 0.5–0.8 BeV. However, previous calculations of the kaon electromagnetic mass difference have typically required cutoffs in the range of 20 BeV and higher.[22] Therefore, the present calculation shows a significant improvement since the cutoff has been reduced to 3.0–3.5 BeV. One might wonder if the inclusion of other s-channel trajectories such as the ones on which the K^* or K_A mesons lie would further decrease this value. Since the present calculation has a change of sign of the mass difference for a cutoff of about 1.5 BeV, it seems doubtful that the inclusion of these other trajectories would reduce the required cutoff to a "reasonable" value.

ACKNOWLEDGMENTS

It is a pleasure to thank Professor K. Tanaka for his advice and encouragement during the course of this investigation. I would also like to thank other members of the Department of Physics, especially Professor R. L. Mills, Professor W. W. Wada, and Dr. E. Y. C. Lu, for many helpful discussions.

[21] M. B. Halpern and G. Segrè, Phys. Rev. Letters **19**, 611 (1967).

[22] The value needed by K. Tanaka in Ref. 10, for example, was about 18 BeV.

PHYSICAL REVIEW VOLUME 187, NUMBER 5 25 NOVEMBER 1969

Theory of Deep-Inelastic Lepton-Nucleon Scattering and Lepton-Pair Annihilation Processes.* I

SIDNEY D. DRELL, DONALD J. LEVY, AND TUNG-MOW YAN
Stanford Linear Acclerator Center, Stanford University, Stanford, California 94305
(Received 20 June 1969)

The structure functions for deep-inelastic lepton processes including (along with other hadron charges and SU_3 quantum numbers) $e^-+p\to e^-+$"anything," $e^-+e^+\to p+$"anything," $\nu+p\to e^-+$"anything," $\bar{\nu}+p\to e^++$"anything" are studied in the Bjorken limit of asymptotically large momentum and energy transfers, q^2 and $M\nu$, with a finite ratio $w\equiv 2M\nu/q^2$. A "parton" model is derived from canonical field theory for all these processes. It follows from this result that all the structure functions depend only on w, as conjectured by Bjorken for the deep-inelastic scattering. To accomplish this derivation it is necessary to introduce a transverse momentum cutoff so that there exists an asymptotic region in which q^2 and $M\nu$ can be made larger than the transverse momenta of all the partons that are involved. Upon crossing to the e^+e^- annihilation channel and deriving a parton model for this process, we arrive at the important result that the deep-inelastic annihilation cross section to a hadron plus "anything" is very large, varying with colliding e^-e^+ beam energy at fixed w in the same way as do point-lepton cross sections. General implications for colliding-ring experiments and ratios of annihilation to scattering cross sections and of neutrino to electron inelastic scattering cross sections are computed and presented. Finally, we discuss the origin of our transverse momentum cutoff and the compatibility of rapidly decreasing elastic electromagnetic form factors with the parton model constructed in this work.

I. INTRODUCTION

THE structure of the hadron is probed by the vector electromagnetic current in the physically observable processes of inelastic electron scattering and of inelastic electron-positron pair annihilation

(i) $e^-+p\to e^-+$"anything,"
(ii) $e^-+e^+\to p+$"anything."

It is also probed by the weak (vector and axial-vector) current in inelastic neutrino or antineutrino scattering

(iii) $\nu_l+p\to +$"anything," $l\equiv e$ or μ
(iv) $\bar{\nu}_l+p\to \bar{l}+$"anything."

In process (i), the scattered electron is detected at a fixed energy and angle, and "anything" indicates the sum over all possible hadron states. The two structure functions summarizing the hadron structure in (i) are

* Work supported by the U. S. Atomic Energy Commission.

defined by

$$W_{\mu\nu}=4\pi^2\frac{E_p}{M}\sum_n\langle P|J_\mu(0)|n\rangle\langle n|J_\nu(0)|P\rangle \times(2\pi)^4\delta^4(q+P-P_n)$$
$$=-\left(g_{\mu\nu}-\frac{q_\mu q_\nu}{q^2}\right)W_1(q^2,\nu)+\frac{1}{M^2}\left(P_\mu-\frac{P\cdot q}{q^2}q_\mu\right)\times\left(P_\nu-\frac{P\cdot q}{q^2}q_\nu\right)W_2(q^2,\nu), \quad (1)$$

where $|P\rangle$ is a one-nucleon state with four-momentum P_μ, $J_\mu(x)$ is the total hadronic electromagnetic current operator, q_μ is the four-momentum of the virtual photon, $q^2\equiv -Q^2<0$ is the square of the virtual photon's mass, and $M\nu\equiv P\cdot q$ is the energy transfer to the proton in the laboratory system. An average over the nucleon spin is understood in the definition $W_{\mu\nu}$. The kinematics are illustrated in Fig. 1. The differential cross section in the rest frame of the target proton is given by

$$\frac{d^2\sigma}{d\epsilon' d\cos\theta}=\frac{8\pi\alpha^2}{(Q^2)^2}(\epsilon')^2[W_2(q^2,\nu)\cos^2(\tfrac{1}{2}\theta)+2W_1(q^2,\nu)\sin^2(\tfrac{1}{2}\theta)], \quad (2)$$

where ϵ and ϵ' are the initial and final energies and θ the scattering angle of the electron.

These structure functions were studied[1] on the basis of canonical field theory in the Bjorken limit[2] of large momentum transfer Q^2 and large energy transfer $M\nu$, with the ratio $w\equiv 2M\nu/Q^2$ fixed. A parton model was derived, and it was shown that in this limit the scattering process viewed from an infinite momentum frame of the proton appears as a superposition of incoherent scatterings of the elementary constituents (partons) of the proton from the bare electromagnetic current. The parton model gives a natural explanation to Bjorken's original suggestion[2] that in the deep inelastic region, W_1 and νW_2 become universal functions of w. It also relates these structure functions to the longitudinal momentum distributions of the elementary constituents of the proton in an infinite-momentum frame, and thereby offers a simple way to study the structure of the proton.[3] A basic ingredient in the derivation of the parton model was the assumption that there exists an asymptotic region in which Q^2 can be made greater than the transverse momenta of all the particles involved, i.e., of the pions and nucleons that are the (virtual) constituents or "partons" of the proton.

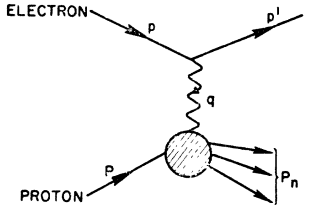

FIG. 1. Kinematics for inelastic electron scattering from a proton.

The crossing properties of field theory or, equivalently, of Feynman graphs relate processes in different channels. It is, therefore, of great interest to study what we can infer from deep-inelastic electron-proton scattering about deep "inelastic" electron-positron annihilation to a proton with fixed momentum (but any polarization) plus "everything else"—i.e., the process (ii). The hadron structure probed in this process is summarized in two structure functions analogous to those in (1) defined by

$$\bar{W}_{\mu\nu}=4\pi^2\frac{E_p}{M}\sum_n\langle 0|J_\mu(0)|Pn\rangle\langle nP|J_\nu(0)|0\rangle \times(2\pi)^4\delta^4(q-P-P_n)$$
$$=-\left(g_{\mu\nu}-\frac{q_\mu q_\nu}{q^2}\right)\bar{W}_1(q^2,\nu)+\frac{1}{M^2}\left(P_\mu-\frac{P\cdot q}{q^2}q_\mu\right)\times\left(P_\nu-\frac{P\cdot q}{q^2}q_\nu\right)\bar{W}_2(q^2,\nu). \quad (3)$$

In (3) a spin average over the detected proton is understood; $q^2>0$ is again the square of the photon's mass and $M\nu\equiv P\cdot q$ is the total energy transfer to hadrons in the rest system of the detected proton. The kinematics for process (ii) are shown in Fig. 2.

One of the primary goals of the present paper is the study of the relation between $\bar{W}_{1,2}$ and $W_{1,2}$. We show in the following that under the same assumptions required in the study of inelastic scattering, the structure functions $\bar{W}_1$ and $\nu\bar{W}_2$ have a Bjorken limit, i.e., they become universal functions of the ratio $2M\nu/q^2$ for large q^2 and $M\nu$. In this limit we can derive a parton model for the $\bar{W}$ from canonical field theory. Furthermore, we also show that the structure functions W_1 and νW_2 for inelastic scattering as measured or calculated near $w\sim 1$ gives predictions to the annihilation process (ii) near $2M\nu/q^2\sim 1$. Since the data on electron-proton scattering from SLAC and DESY[4] seem to support at least qualitatively Bjorken's original suggestion, we reach the important conclusion that the structure functions $\bar{W}_1$ and $\nu\bar{W}_2$ should also be expected to exhibit similar universal behavior at high energies

[1] S. D. Drell, D. Levy, and T. M. Yan, Phys. Rev. Letters **22**, 744 (1969).

[2] J. D. Bjorken, Phys. Rev. **179**, 1547 (1969).

[3] This connection was first noted by R. P. Feynman (unpublished), who also invented the term "parton." A partonlike model was also suggested by J. D. Bjorken, in *Proceedings of the International School of Physics "Enrico Fermi": Course XLI*, edited by J. Steinberger (Academic Press Inc., New York, 1968). See also J. D. Bjorken and E. A. Paschos, Phys. Rev. **185**, 1975 (1969).

[4] E. Bloom *et al.*, quoted in W. K. H. Panofsky, *Proceedings of the Fourteenth International Conference on High-Energy Physics, Vienna, 1968*, edited by J. Prentki and J. Steinberger (CERN, Geneva, 1968), p. 23; W. Albrecht *et al.*, DESY Report No. 69/7 (unpublished).

with the structure functions for annihilation closely related to those for scattering. The precise connection is given in Sec. III.

The kinematical region for (ii) in the q^2, $M\nu$ plane is bounded as follows: For a fixed collision energy $q^2>4M^2$ the value of ν is bounded below by $\nu_{\min}=\sqrt{(q^2)}$, corresponding to the detected proton at rest in the center-of-mass or the colliding ring system, and is bounded above by $2M\nu_{\max}=q^2$, corresponding to the "elastic" process $e^-+e^+\rightarrow p+\bar{p}$. Thus $0<2M\nu/q^2<1$ for process (ii). We recall that for inelastic electron-proton scattering $1<2M\nu/Q^2<\infty$. For convenience the same symbol w is used to denote $2M\nu/q^2$ for annihilation and $2M\nu/Q^2$ for scattering. The limit $w=1$ corresponds to the elastic processes $e+p\rightarrow e'+p'$ in scattering and $e^-+e^+\rightarrow p+\bar{p}$ in annihilation. Since we are interested in the deep-inelastic continuum and not the resonance excitations, we require $2M\nu-Q^2\gg M^2$ for scattering and $q^2-2M\nu\gg M^2$ for annihilation, i.e., we always assume $|q^2(w-1)|\gg M^2$. The point $w=1$ will only be approached from both sides. The regions of the $(q^2, 2M\nu)$ plane corresponding to physical scattering and annihilation processes are shown in Fig. 3. Our results enable us to predict the structure functions and hence the annihilation cross section that can be studied near $w=1$ by colliding rings now under construction. In the colliding-ring or center-of-mass frame, the differential cross section for (ii) is given by

$$\frac{d^2\sigma}{dE\,d\cos\theta}=\frac{4\pi\alpha^2}{(q^2)^2}\frac{M^2\nu}{\sqrt{q^2}}\left(1-\frac{q^2}{\nu^2}\right)^{1/2}\left[2\bar{W}_1(q^2,\nu)+\frac{2M\nu}{q^2}\left(1-\frac{q^2}{\nu^2}\right)\frac{\nu\bar{W}_2(q^2,\nu)}{2M}\sin^2\theta\right], \quad (4)$$

where E is the energy of the detected proton, and θ is the angle of the proton momentum $\mathbf{P}$ with respect to the axis defined by the incident colliding e^- and e^+ beams.

For the weak-interaction processes (iii) and (iv), the kinematics are identical with the inelastic electron scattering (i) when we neglect the lepton rest masses. Additional structure functions appear as a result of the parity nonconservation in the weak interactions. For process (iii), Eq. (1) is replaced by

$$W_{\mu\nu}'=4\pi^2\frac{E_p}{M}\sum_n\langle P|J_\mu{}^{c\dagger}(0)|n\rangle\langle n|J_\nu{}^c(0)|P\rangle\times(2\pi)^4\delta^4(q+P-P_n)$$
$$=-g_{\mu\nu}W_1'(q^2,\nu)+(1/M^2)P_\mu P_\nu W_2'(q^2,\nu)+i(\epsilon_{\mu\nu\sigma\tau}P^\sigma q^\tau/2M^2)W_3'(q^2,\nu)+\cdots, \quad (5)$$

where $J_\mu{}^c(x)$ is the Cabibbo current describing hadronic weak interactions. The dots denote additional terms proportional to q_μ or q_ν which, therefore, do not contribute to the inelastic scattering because of conservation

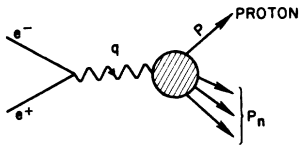

FIG. 2. Kinematics for inelastic electron-positron annihilation leading to a proton.

of the lepton current. The inelastic scattering cross section is given by

$$\frac{d^2\sigma^\nu}{d\epsilon'\,d\cos\theta}=\frac{G^2}{\pi}(\epsilon')^2\left[W_2'(q^2,\nu)\cos^2(\tfrac{1}{2}\theta)+2W_1'(q^2,\nu)\times\sin^2(\tfrac{1}{2}\theta)+W_3'(q^2,\nu)\sin^2(\tfrac{1}{2}\theta)\left(\frac{\epsilon+\epsilon'}{M}\right)\right]. \quad (6)$$

In the Bjorken limit, a parton model can be derived again from canonical field theory. With specific theories and the conserved-vector-current hypothesis, the W_1' and $\nu W_2'$ can be related to W_1 and νW_2, respectively, and the behavior of W_3' can be predicted. This leads to specific and significant predictions for the ratio of neutrino to electron inelastic cross sections as well as for the difference between neutrino and antineutrino inelastic cross sections, (iii) and (iv), in the deep inelastic region.

In this first of a series of papers we place primary emphasis on the general ideas and assumptions in our program of deriving the Bjorken limit for the inelastic structure functions, i.e., the "parton" model, from canonical field theory. In Sec. II we first amplify and clarify the derivation of the parton model given in Ref. 1 (and correct the discussion presented there). In Sec. III we accomplish the crossing to the annihilation process (ii) and derive the parton model for the structure functions $\bar{W}_1$ and $\nu\bar{W}_2$. Experimental predictions are also given. In Sec. IV we extend our work to the Cabibbo currents and weak interactions. Subsequent papers will enter systematically into full calculational details of all derivations and assumptions.

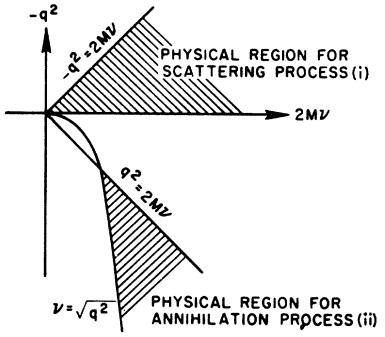

FIG. 3. Physical regions in the $(-q^2, 2M\nu)$ plane corresponding to inelastic scattering from a proton and to e^-e^+ annihilation to a proton.

II. DEEP-INELASTIC ELECTRON SCATTERING

In this section we review and clarify the general arguments in the derivation of the parton model for inelastic scattering.[5] We perform our calculations in the infinite-momentum center-of-mass frame of the electron and proton, where

$$q^0=\frac{2M\nu-Q^2}{4P},\quad q_3=\frac{-2M\nu-Q^2}{4P},\quad |\mathbf{q}_\perp|=\sqrt{(Q^2)}+O(1/P^2), \tag{7}$$

with the nucleon momentum $\mathbf{P}$ along the 3 axis. We undress the current operator and go into the interaction picture with the familiar U-matrix transformation

$$J_\mu(x)=U^{-1}(t)j_\mu(x)U(t), \tag{8}$$

where $J_\mu(x)$ is the fully interacting electromagnetic current, and $j_\mu(x)$ is the corresponding free or bare current. Equation (1) can now be rewritten as

$$W_{\mu\nu}=4\pi^2\frac{E_p}{M}\sum_n\langle UP|j_\mu(0)U(0)|n\rangle\langle n|U^{-1}(0)j_\nu(0)|UP\rangle \times(2\pi)^4\delta^4(q+P-P_n), \tag{9}$$

where $|UP\rangle=U(0)|P\rangle$.

A basic ingredient in the derivation of the parton model from canonical field theory is the existence of an asymptotic region in which Q^2 can be made greater than the transverse momenta of all the particles involved, i.e., of the pions and nucleons that are the (virtual) constituents of $|UP\rangle$. We must *assume* the existence of such a region in our formal theoretical manipulations. Such an assumption is in agreement with present high-energy data that strongly indicate that transverse momenta of the final particles are indeed very limited in magnitude. The $U(0)$'s adjacent to the final states $|n\rangle\langle n|$ may be replaced by unity in the Bjorken limit as we now show. Although we claimed this in Ref. 1, the compressed statement of the argument presented there in the paragraph following Eq. (8) was incomplete and failed to establish this claim.

Under the fundamental assumption that the particles emitted or absorbed at any strong vertex have only finite transverse momenta, both $U|P\rangle$ and $U|n\rangle$ can be treated as eigenstates of the Hamiltonian with eigenvalues E_p and E_n, respectively. To show this, let E_{up} symbolically denote the energy of one of the multipion+nucleon states in the perturbation expansion of $|UP\rangle$. In the infinite momentum frame, E_p-E_{up} is of the order of $1/P$ multiplied by the sum of squares of some characteristic transverse momentum and some characteristic mass. For example, let $|UP\rangle$ denote a state of one nucleon with momentum $\eta\mathbf{P}+\mathbf{k}_\perp$ plus one pion with $(1-\eta)\mathbf{P}-\mathbf{k}_\perp$ in accord with momentum conservation; and $\mathbf{k}_\perp\cdot\mathbf{P}=0$. We also take the fraction of momentum carried by the nucleon and pion lines, respectively, η and $(1-\eta)$, to be positive along the $\mathbf{P}$ direction. The kinematics are shown in Fig. 4. We find then, for $P\to\infty$,

$$E_p-E_{up}=\left(P+\frac{M^2}{2P}\right)-\left(\eta P+\frac{k_\perp^2+M^2}{2\eta P}\right)-\left((1-\eta)P+\frac{k_\perp^2+\mu^2}{2(1-\eta)P}\right)=\frac{-1}{2P}\left(\frac{k_\perp^2}{\eta(1-\eta)}+\frac{M^2(1-\eta)}{\eta}+\frac{\mu^2}{(1-\eta)}\right). \tag{10}$$

This difference in (10) will generally be negligible[6] in comparison with the photon energy q^0 as given in (7) and, therefore, can be neglected in the energy δ function $\delta(q_0+E_p-E_n)$ appearing in (9), provided we work in the Bjorken limit $2M\nu-Q^2\gg M^2$ and we restrict $(k_\perp)_{\max}^2\ll Q^2$. This argument fails for the regions of momenta $\eta<0$ or >1 which lead to $E_{up}-E_p\sim P$, corresponding to particles moving antiparallel as well as parallel to $\mathbf{P}$. However, by analyses such as described by Weinberg[7] we establish that for these regions of η the energy denominators introduced by the time integrals appearing in the expansion of the time-ordered products of

$$U(0)\equiv\left[\exp\left(-i\int_{-\infty}^{0}H_I(\tau)d\tau\right)\right]_+ \tag{11}$$

lead to contributions to $W_{\mu\nu}$ reduced by factors of $\sim 1/P$. This analysis is spelled out in detail in the following paper. In particular, we must work only with the good components of the current, i.e., J_μ for $\mu=0$ or 3 along the direction of $\mathbf{P}$. Otherwise, the diagrams with particles moving with $\eta<0$ or >1 cannot be excluded, because the extra powers of P in the denominator can be compensated by similar factors in the numerator from matrix elements of the bad components of the current, that is, J_1 and J_2 in the $P_3\to\infty$ frame. However, we can compute the contributions of the good components only—i.e., W_{00} and W_{33}—and by covariance construct the whole tensor.

Having shown that both $U|P\rangle$ and $U|n\rangle$ can be treated as eigenstates of the total Hamiltonian with eigenvalues E_p and E_n, respectively, in the limit Q^2,

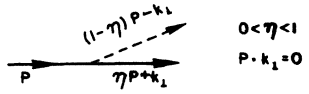

FIG. 4. Diagram for the emission of a pion (dashed line) from a nucleon (solid line) with the momentum labels as indicated.

[5] The brief discussion given in Ref. 1 contains incorrect statements. The derivation given in this paper serves as a clarification. However, none of the results presented in Ref. 1 is affected.

[6] Detailed calculations verify that the extreme end regions $\eta\sim M^2/Q^2$ and $\eta\sim 1-M^2/Q^2$ contribute negligibly.

[7] S. Weinberg, Phys. Rev. **150**, 1313 (1966).

$M\nu \to \infty$, the over-all energy-conserving δ function in (9) can be replaced by the energy-conserving δ function across the electromagnetic vertex. One can then make use of the translation operators, completeness of states n, and the unitarity of the U matrix to obtain the parton-model result. We illustrate these steps in the following operations on (9):

$$\lim_{P\to\infty;\, q^2, M\nu\to\infty;\, w \text{ fixed}} W_{\mu\nu}$$

$$= 4\pi^2 \frac{E_p}{M} \sum_n \int (dx) e^{+iqx} \langle UP | j_\mu(x) U(0) | n\rangle \times \langle n | U^{-1}(0) j_\nu(0) | UP\rangle$$

$$= 4\pi^2 \frac{E_p}{M} \int (dx) e^{+iqx} \langle UP | j_\mu(x) U(0) U^{-1}(0) j_\nu(0) | UP\rangle$$

$$= 4\pi^2 \frac{E_p}{M} \int (dx) e^{+iqx} \langle UP | j_\mu(x) j_\nu(0) | UP\rangle. \qquad (12)$$

It is useful to understand the physics behind this derivation. Consider $\langle UP | j_\mu(0) U(0) | n\rangle$. Before the electromagnetic current operates, $\langle UP|$ describes emission and reabsorption of pions and nucleon-antinucleon pairs. All these particles form a group moving very close to each other along the direction $\mathbf{P}$, the momentum of the proton. The free or bare current scatters one of these constituents and imparts to it a very large transverse momentum $|\mathbf{q}_\perp| \simeq \sqrt{(Q^2)}$. This scattered particle emits and reabsorbs pions and nucleon-antinucleon pairs. They form a second group moving close to each other but along a direction which deviates in transverse momentum by $\mathbf{q}_\perp$ from the first group, as illustrated in Fig. 5. In the lab frame this looks as follows: The constituents of the proton in group (B) of Fig. 5 emerge with very high momenta along $\mathbf{q}$, while the rest in group (A) are left behind.

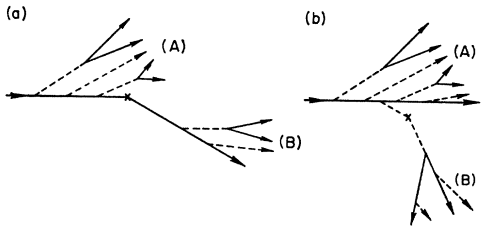

FIG. 5. Diagram illustrating pions and nucleons moving in well-separated and well-identified groups along the directions $\mathbf{P}$ and $\eta\mathbf{P}+\mathbf{q}$. This illustrates the effect of the transverse-momentum cutoff and the meaning of an asymptotic region in our model.

The invariant mass of each of the two groups is small, since the transverse momenta of the constituents do not spread far away from each other. The energy differences between $|P\rangle$ and $|UP\rangle$, $|n\rangle$ and $U(0)|n\rangle$ are, therefore, negligible in the limit of large Q^2 and $M\nu$. Furthermore, as $Q^2 \to \infty$, there is no interference between the two groups of particles. The U matrix acts separately and independently on each of the two groups (A) and (B) in Fig. 5. Our derived result simply states the fact that the total probability that anything happens among the particles in each of the two groups (A) and (B) is unity because of unitarity of the U matrix.[8] An example of this result, $U|n\rangle \to |n\rangle$, is illustrated by the graphs in Fig. 6.

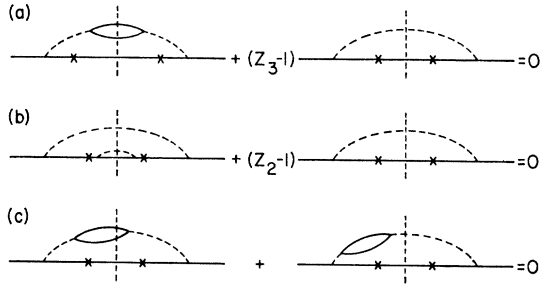

FIG. 6. Examples of graphs in a fourth-order calculation that add to zero, indicating that the total effect of U operating on states $|n\rangle$ *after* the interaction with the electromagnetic current, represented by the $\times$, can be replaced by unity—i.e., $U|n\rangle \to |n\rangle$. The graphs picture the square of the matrix element; the vertical dashed line signifies that we are computing only the absorptive part describing production of real final states that are formed upon interaction of the proton with the current. The vertices are time-ordered, with time increasing to the right (left) for interactions to the left (right) of the dashed line.

The result of Eq. (12) establishes the "parton model" by allowing us to work with free point currents and the superposition of essentially free (i.e., long-lived) constituents in describing the proton's ground state in the infinite momentum frame and in the Bjorken limit.

In particular, the form of (12) assures us that if the bare current $j_\mu(x)$ lands on a constituent in $|UP\rangle$ with momentum P_a, $P_a{}^2 \cong M_a{}^2$, it scatters it on to the mass shell with P_a+q and $(P_a+q)^2 \cong M_a{}^2$. By simple integration of (12), this mass-shell constraint emerges as a δ function,

$$\delta(2P_a\cdot q - Q^2) \cong \delta(2\eta M\nu - Q^2) = (1/2M\nu)\delta(\eta - 1/w), \quad (13)$$

where we have used (7), and η is the fraction of longitudinal momentum born by the constituent on which the bare current lands. Equation (13) leads to a universal behavior of W_1 and νW_2 as a function of w, as predicted by Bjorken and illustrated in Ref. 1, and shows that the observed w dependence reflects the longitudinal momentum distribution of the constituents in the infinite-momentum frame.

The detailed calculations of the functional forms for W_1 and νW_2 as worked out in Ref. 1 for large $w \gg 1$ will also be presented in the following paper.

It remains for us only to verify that the result presented by (12) is actually finite and nonvanishing—i.e., to show that we have actually retained the leading contribution in the Bjorken limit. We do this by the

[8] The unitarity of the U matrix is preserved even though we use a cutoff procedure which has to be properly defined in detail, as is displayed explicitly in the derivations presented in the following paper.

following construction. We expand $|UP\rangle$ in terms of a complete set of multiparticle states

$$|UP\rangle=\sum_n a_n|n\rangle, \quad \sum_n|a_n|^2=1.$$

Introducing this into (12), we use the following relation to identify W_2, the coefficient of $P_\mu P_\nu$:

$$\int(dx)e^{iqx}\langle P_{n,i}|j_\mu(x)j_\nu(0)|P_{n,i}\rangle$$
$$=\frac{1}{4\pi^2}\frac{1}{E_{n,i}}2P_{n,\mu}P_{n,\nu}\delta(Q^2-2M\nu\eta_{n,i})+\cdots$$
$$=\frac{P_\mu P_\nu}{4\pi^2 P}\frac{1}{M\nu w}\delta\left(\eta_{n,i}-\frac{1}{w}\right)+\cdots.$$

$P_{n,i}$ is the four-momentum of the charged constituent on which the current lands, and $\eta_{n,i}$ has the same meaning as the η in (13); the dots indicate the additional contributions to the structure function W_1. The charged constituent can be a $\pi^\pm$, p, or $\bar{p}$. For the nucleon current the above equation follows from the use of projection matrices $M+\gamma P_n$ and $M+\gamma(P_n+q)$ before and after the current acts. Then symbolically we have

$$\nu W_2=\frac{1}{w}\sum_n|a_n|^2[\langle n|\sum_i\delta(\eta_{n,i}-1/w)\lambda_{n,i}^2|n\rangle/\langle P|P\rangle],$$

where $\lambda_{n,i}$ is the charge of the ith constituent in state $|n\rangle$. This relation gives a sum rule

$$\int_1^\infty\frac{dw}{w}(\nu W_2)=\sum_n(\sum_i\lambda_{n,i}^2)|a_n|^2$$
$$=\sum_n n_c|a_n|^2,$$

where n_c is the number of charged constituents in state $|n\rangle$. We have here implicitly assumed that the constituents are all integrally charged, as is the case in our model. Thus, the weighted integral of νW_2 over w may be interpreted as the mean number of charged constituents in the physical proton. It follows from $n_c\geq 1$ and the normalization condition of a_n's that

$$\int_1^\infty\frac{dw}{w}(\nu W_2)\geq 1. \tag{14}$$

This inequality is trivial to satisfy if the SLAC data continue their present trend, since νW_2 appears to be approximately constant for large w.

III. CROSSING AND DEEP-INELASTIC ELECTRON-POSITRON ANNIHILATION

The crossing properties of field theory, or, equivalently, of the individual Feynman amplitudes, relate processes such as (i) with a proton in the initial state to the corresponding process with an emerging antiproton in the final state. Unless we want to entertain the possibility of C, or T, violation in the hadronic electromagnetic interactions, we can equally well talk about an emerging proton, or antiproton, in the final state[9] of (ii).

By straightforward application of the reduction formalism to the proton with four-momentum P in the states in (1) and (3), it is readily shown that $W_{\mu\nu}$ and $\bar{W}_{\mu\nu}$ are related by the substitution law

$$\begin{aligned}\bar{W}_{\mu\nu}(q,P)&=-W_{\mu\nu}(q,-P),\\ \bar{W}_1(q^2,\nu)&=-W_1(q^2,-\nu),\\ \nu\bar{W}_2(q^2,\nu)&=(-\nu)W_2(q^2,-\nu).\end{aligned} \tag{15}$$

We write for spacelike q^2

$$MW_1(q^2,\nu)=F_1(w,s), \quad \nu W_2(q^2,\nu)=F_2(w,s),$$

where $w\equiv 2M\nu/(-q^2)>1$ and $s\equiv(q+P)^2=2M\nu-Q^2+M^2>M^2$. In the Bjorken limit ($\lim_{\mathrm{Bj}}$), we have

$$\begin{aligned}\lim_{\mathrm{Bj}}MW_1(q^2,\nu)&=F_1(w)=\lim_{s\to\infty}F_1(w,s) \quad (w>1)\\ \lim_{\mathrm{Bj}}\nu W_2(q^2,\nu)&=F_2(w)=\lim_{s\to\infty}F_2(w,s) \quad (w>1).\end{aligned} \tag{16}$$

The substitution law (15) gives for timelike q^2

$$M\bar{W}_1(q^2,\nu)=-F_1(w,s), \quad \nu\bar{W}_2(q^2,\nu)=F_2(w,s), \tag{17}$$

where $0<w=2M\nu/q^2<1$ and $s=(q-P)^2=q^2-2M\nu+M^2>M^2$. If we can show that the Bjorken limit exists for timelike q^2, we expect to find in general

$$\begin{aligned}\lim_{\mathrm{Bj}}(-)M\bar{W}_1(q^2,\nu)&=\bar{F}_1(w)=\lim_{s\to\infty}F_1(w,s)=F_1(w),\\ \lim_{\mathrm{Bj}}\nu\bar{W}_2(q^2,\nu)&=\bar{F}_2(w)=\lim_{s\to\infty}F_2(w,s)=F_2(w),\end{aligned} \tag{18}$$

namely, $\bar{F}_1(w)$ and $\bar{F}_2(w)$ are the continuations of the corresponding functions $F_1(w)$ and $F_2(w)$ from $w>1$ to $w<1$. Relations (18) will be true, for example, if the Bjorken limits are approached algebraically so the sign change in $w-1$ between $w>1$ for scattering and $0<w<1$ for pair annihilation will not have any pathological effect. We now demonstrate, using as an example the model developed in Ref. 1 of charge-symmetric theory of pseudoscalar pions and nucleons with γ_5 coupling and with a transverse momentum cutoff, that first, the Bjorken limits of $\bar{W}_1$ and $\nu\bar{W}_2$ exist, and second, the relations (18) are indeed satisfied.

A convenient infinite-momentum frame for this analysis is one in which

$$\begin{aligned}q^\mu&=(q_3+q^2/2q_3,\,0,\,0,\,q_3),\\ P^\mu&=(P+M^2/2P,\,0,\,0,\,P).\end{aligned} \tag{19}$$

[9] This means that such a difference should be probed for experimentally. If one is found, we would have to rule out the possibility that it is due to higher-order electromagnetic contributions before interpreting it as C violation.

For large $q^2 \gg M^2$ we have, since $q \cdot P \equiv M\nu$,

$$q_3 = (q^2/2M\nu)P = (1/w)P. \tag{20}$$

In analogy to our discussion of (i), we undress the current by substituting (8) into (3). There is an immediate simplification if we restrict ourselves to studying the good components of J_μ ($\mu=0$ or 3). For these components, we can ignore the $U(0)$'s acting on the vacuum, and obtain from (8)

$$\bar{W}_{\mu\nu} = 4\pi^2 \frac{E_p}{M} \sum_n \langle 0|j_\mu(0)U(0)|Pn\rangle\langle nP|U^{-1}(0)j_\nu(0)|0\rangle \times (2\pi)^4\delta^4(q-P-P_n). \tag{21}$$

The reason for this simplification is similar to that mentioned below (11) in connection with the inelastic scattering. If $U(0)$ operates on the vacuum state, it must produce a baryon pair plus meson with zero total momentum so that at least one particle will move toward the left and another toward the right along $\mathbf{q}$ or $\mathbf{P}$ in (3). Thus the energy denominators will be of order $\sim P$ instead of $\sim 1/P$ as in (10). However, when working with the good components of the current—i.e., J_0 or J_3 along $\mathbf{P}$, no compensating factors of P are introduced into the numerator by the vertices, and so such terms can be neglected in the infinite-momentum limit. The detailed systematic writing of this analysis appears in a subsequent paper.

Continuing in parallel with the discussion of inelastic scattering, we make the same fundamental assumption that there exists a transverse momentum cutoff at any strong vertex. Equation (21) says that the first thing that happens is the creation of a pion pair or of a proton-antiproton pair. In the limit of large q^2, energy-momentum conservation forces at least one energy denominator in the expansion of $U(0)$ in the old-fashioned perturbation series to be of order $q^2 \gg M^2$ or $k_\perp^2$ for diagrams involving interactions between the two groups of particles, the one group created by one member of the pair and the other group created by the other member of the pair produced by j_μ. Therefore contributions of these diagrams illustrated in Fig. 7 vanish as $q^2 \to \infty$. Diagrams with different pairs created at the two electromagnetic vertices as in Fig. 7 also vanish by similar reasoning. In complete analogy to the scattering problem as discussed around (10), the state $U(0)|Pn\rangle$ may be treated as an eigenstate of the total Hamiltonian with eigenvalue E_p+E_n. Thus Eq. (21) can be written with the aid of the translation operators as

$$\bar{W}_{\mu\nu} = 4\pi^2 \frac{E_p}{M} \int (dx) e^{+iqx} \sum_n \langle 0|j_\mu(x)U(0)|Pn\rangle \times \langle nP|U^{-1}(0)j_\nu(0)|0\rangle. \tag{22}$$

A simple kinematical consideration reveals that most of the longitudinal momentum of the virtual photon is

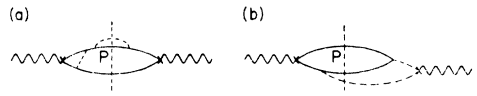

FIG. 7. Examples of diagrams whose contributions vanish as $q^2 \to \infty$.

given to that particle in the pair produced from the vacuum by j_μ which will eventually create the detected proton of momentum $\mathbf{P}$. As an example, consider the second-order diagram with the pion current operating as in Fig. 8(a) [Fig. 8(b) is its parallel in the inelastic scattering]. The contribution of this diagram to $\bar{W}_{\mu\nu}$ according to the charge-symmetric γ_5 pion-nucleon canonical field-theory model of Ref. 1 is

$$\bar{W}_{\mu\nu} = \frac{g^2}{(2\pi)^3}\frac{1}{2M}\int \frac{d^3P_{\bar{n}}}{2E_{\bar{n}}}\frac{1}{2\omega_-}\delta(q^0-E_p-E_{\bar{n}}-\omega_-) \times 4k_{+\mu}k_{+\nu}\frac{\mathrm{Tr}\{(M-\gamma P)(M-\gamma P_{\bar{n}})\}}{(2\omega_+)^2(E_p+E_{\bar{n}}-\omega_+)^2}. \tag{23}$$

The notations used here are self-explanatory; in particular we use $q_3=(1/\omega)P$ by (20). In terms of the momentum parametrizations indicated in Fig. 8, the solution to the energy-conserving δ function in (23) is

$$\eta = \frac{1}{w} + \left(\frac{k_\perp^2}{2M\nu}\right) \to \frac{1}{w} \quad \text{as} \quad 2M\nu \to \infty.$$

Hence by (20),

$$\mathbf{k}_+ = \eta\mathbf{P} + \mathbf{k}_\perp = \mathbf{q}_3 + \mathbf{k}_\perp$$

and

$$\mathbf{k}_- = (1/w-\eta)\mathbf{P} - \mathbf{k}_\perp \sim (k_\perp^2/q^2)\mathbf{q}_3 - \mathbf{k}_\perp,$$

which verifies our assertion. Thus the virtual photon creates two distinct groups of particles with no interactions between the two. The group which contains the detected proton moves with almost all of the longitudinal momentum q_3, while the other group moves with a very small fraction $\sim(k_\perp^2/q^2)q_3$. Again the U matrix acts on the two groups separately and independently. We can sum over all possible combinations of particles in the small momentum group to obtain unity for the total probability for anything to happen. In other words, in Eq. (22) we have retained only those terms in which the small momentum group involves only one charged particle ($\pi^\pm$, P or $\bar{P}$), which we shall

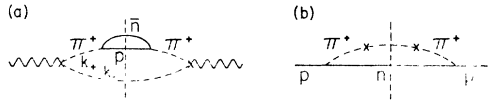

FIG. 8. Second-order diagrams with the current interacting on the pion line, (a) for pair annihilation and (b) for scattering.

denote by λ. Therefore

$$\bar{W}_{\mu\nu}=4\pi^2\frac{E_p}{M}\int(dx)e^{+iqx}\sum_{n,\lambda=\pm}\langle 0|j_\mu(x)|\lambda,U^{-1}(0)(Pn)\rangle \times\langle(nP)U^{-1}(0),\lambda|j_\nu(0)|0\rangle, \quad (24)$$

which is the analog of (12). Notice that in the Bjorken limit, the same classes of diagrams contribute to ep scattering and annihilation process.

Although it is not apparent that $\bar{F}_1(w)$ and $\bar{F}_2(w)$ computed from (24) are the same as $F_1(w)$ and $F_2(w)$ computed from (12) and continued to $0<w<1$, it is actually so by explicit calculation. Verification is trivial for second-order pion current contributions and for the ones for nucleon current contributions similar to Fig. 8. In particular, (23) gives

$$\nu\bar{W}_2=\frac{g^2}{8\pi^2}\frac{1}{w^2}\ln\left\{1+\frac{k_{1\max}^2}{M^2}\left[\frac{1}{w^2}+\frac{\mu^2}{M^2}\left(1-\frac{1}{w}\right)\right]^{-1}\right\}. \quad (25)$$

We have also verified this explicitly to fourth order in g for diagrams with both pion and nucleon current contributions, and to any order for ladder diagrams with the nucleon current operating [Fig. 9 and its corresponding diagram for annihilation process (ii)]. In this verification, we only have to identify the transverse momentum cutoffs in both cases.

We can now study the experimental implications of (18). In the Bjorken limit, (4) becomes, using $E=M\nu/q^0=M\nu/\sqrt{(q^2)}$ and the definition $w=2M\nu/q^2$,

$$d^2\sigma/dwd\cos\theta=\tfrac{3}{2}\sigma_l[-F_1(w)+\tfrac{1}{4}wF_2(w)\sin^2\theta]w, \quad (26)$$

where

$$\sigma_l=\tfrac{1}{3}(4\pi\alpha^2/q^2)$$

is the total cross section of electron-positron annihilation into muon pairs, in the relativistic limit. Generally, knowledge about $F_{1,2}(w)$ for $w>1$ as determined by inelastic ep scattering measurements does not provide any useful information for $0<w<1$ unless one knows the analytic forms of $F_{1,2}(w)$ exactly. However, $w=1$ is a common boundary for both scattering and annihilation. Therefore, with a mild assumption of smoothness, the ep deep-inelastic scattering data near $w\gtrsim 1$ predict completely the "deep" inelastic annihilation process

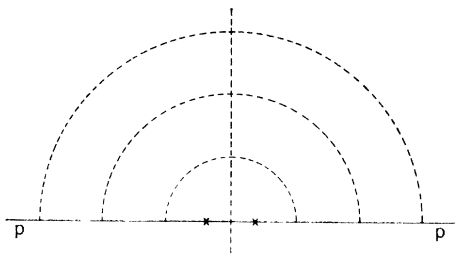

FIG. 9. Dominant ladder diagrams for large w as computed in Ref. 1.

(ii) near $w\lesssim 1$. This connection is a far-reaching consequence of the Bjorken limit. The two processes occur in different and disjoint kinematical regions and are not related in general. Recall that $w=1$ corresponds to the two-body elastic channel, and by w near 1 we mean $|q^2(w-1)|\gg M^2$.

In (26), we may choose $\sin^2\theta=0$; thus it is necessary that

$$F_1(w)\leq 0, \quad 0<w<1. \quad (27)$$

It can be readily verified that for any value of w, if the interaction of the current is with the nucleon,

$$F_1(w)=\tfrac{1}{2}wF_2(w), \quad j_\mu=\bar{\psi}_P\gamma_\mu\psi_P;$$

and if it is with the pion,

$$F_1(w)=0, \quad j_\mu=i\pi^+\overleftrightarrow{\partial}_\mu\pi^-.$$

On the other hand, $F_{1,2}(w)$ are non-negative for $w>1$. We conclude that both $F_1(w)$ and $F_2(w)$ change sign at $w=1$ if the nucleon current dominates, while $F_2(w)$ does not change sign at $w=1$ if the pion current dominates. We therefore predict near $w\sim 1$ that

$$\begin{aligned}&F_2(w)=C_N(w-1)^{2n+1}, \quad n=0,1,\ldots \text{ (nucleon current)},\\ &F_2(w)=C_\pi(w-1)^{2n}, \quad n=0,1,\ldots \text{ (pion current)}.\end{aligned} \quad (28)$$

We are not able to perform a reliable calculation near $w\simeq 1$ from our field-theoretical model, since the virtual particles involved are very virtual, and the off-shell effects must be correctly taken into account. This is in contrast to our results in Ref. 1 for large $w\gg 1$, where we found the intermediate particles to be close to their energy shells and the vertex and self-energy corrections to contribute lower powers of $\ln w\gg 1$ for each order of g^2. However, a plausible conjecture can be made. Diagrams without strong vertex corrections properly included indicate that the pion current gives the dominant contribution near $w\sim 1$. For example, to lowest order in g^2, we find near $w\gtrsim 1$ from (25) for the pion current, and from a similar expression for the nucleon-current contribution that

$$\begin{aligned}&F_2(w)\cong(g^2/16\pi^2)\ln[1+k_{1\max}^2/\mu^2](w-1) \text{ (nucleon current)},\\ &F_2(w)\cong(g^2/8\pi^2)\ln[1+k_{1\max}^2/M^2] \text{ (pion current)}.\end{aligned} \quad (29)$$

The virtual particle (a proton in the first case and a pion in the second) has a large (spacelike) invariant mass proportional to $k_1^2/(w-1)$. If a form factor is included at each of the two pion-nucleon vertices as illustrated in Fig. 10, (29) becomes

$$\begin{aligned}&F_2\propto(w-1)F_p^2\left(\frac{C}{w-1}\right) \text{ (nucleon current)},\\ &F_2\propto F_\pi^2\left(\frac{C'}{w-1}\right) \text{ (pion current)},\end{aligned} \quad (30)$$

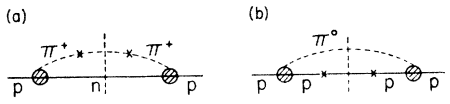

FIG. 10. Diagrams with *ad hoc* form factors inserted at the pion-nucleon vertices to dampen the amplitude when the virtual pion (a) or nucleon (b) is very virtual.

The subscripts p or π at the squares of the pion-nucleon form factors indicate the particle which is virtual. If F_p and F_π behave similarly for large momentum transfers, then the pion current will continue to dominate with one less power of $(w-1)$ as $w \to 1$ when the vertex corrections are included. On the basis of our conjecture, we interpret $F_2(w)$ near $w \sim 1$ as a measure of the asymptotic pion-nucleon form factor. Available data from SLAC[10] are consistent with the fit

$$F_2(w) \approx C_1(w-1)^2, \quad w \gtrsim 1$$

indicating that, if our conjecture that the pion current dominates in the threshold region is correct, the pion-nucleon form factor decreases with the first inverse power of invariant momentum transfer squared—a result we consider as reasonable.

We want to emphasize that independent of this specific conjecture based on our model, it follows from the existence of a Bjorken limit that the deep annihilation cross section varies with total energy of the colliding electron-positron system as $1/q^2$, just the same as the cross section for a point hadron. Furthermore, even without calculating the specific values of $F_{1,2}(w)$ from a theory, one can predict from (26) plus the observed structure functions for inelastic scattering that there will be a sizable cross section and many interesting channels to study in the deep-inelastic region of colliding e^-e^+ beams. Moreover, the distribution of secondaries in the colliding ring frame will look like two jets with typical transverse momenta $k_\perp \ll \sqrt{(q^2)}$ on the individual particles. The relative roles of the nucleon and pion currents can be studied by separating $F_1(w)$ from $F_2(w)$, or $\bar{W}_1$ from $\nu\bar{W}_2$ by the angular distribution in (26).

Three further observations are worth noting:

(1) By detecting different baryons in the final states, one has a simple test of the unitary symmetry scheme of strong interactions. For example, according to SU_3 and the hypothesis that the electromagnetic current is a U-spin singlet, the differential cross sections labeled by the detected baryon and observed at identical values of q^2 and $q \cdot P$ should satisfy the relations

$$\sigma_{\Xi^-} = \sigma_{\Sigma^-}, \quad \sigma_{\Sigma^+} = \sigma_p,$$
$$\sigma_{\Xi^0} = \sigma_n = \tfrac{1}{2}(3\sigma_\Lambda - \sigma_{\Sigma^0}).$$

Similar relations can be written for the mesons with an added constraint due to the fact that π^- and π^+ are each other's antiparticles; thus

$$\sigma_{\pi^-} = \sigma_{K^-} = \sigma_{\pi^+} = \sigma_{K^+},$$
$$\sigma_{K^0} = \sigma_{\bar{K}^0} = \tfrac{1}{2}(3\sigma_\eta - \sigma_{\pi^0}).$$

This should be an ideal place to test SU_3 relations, since the mass differences among members of a multiplet should have a negligible effect on the dynamics as well as the kinematics in these regions of asymptotically large momentum and energy transfers.

(2) If charge conjugation is a good symmetry of the electromagnetic interactions, the differential cross sections for detecting a particle or its antiparticle are identical. According to (26), the differential cross section for (ii) as a function of q^2 is comparable in magnitude to that for lepton-pair creation and very much larger than the observed "elastic" annihilation process from a $p\bar{p}$ pair. Consequently, it should be feasible by detecting and comparing charge-conjugate states, such as Λ and $\bar{\Lambda}$, for example, to test charge-conjugation conservation in electromagnetic interactions of hadrons.[11]

(3) Finally, the reader may wonder what are the implications of this model and the existence of a Bjorken limit for e^-e^+ annihilation to form a deuteron (or any other "composite" system in place of the proton) plus anything. These are best illustrated by considering the deuteron and noting that the kinematically allowed regions are the same as illustrated in Fig. 3, but with the mass M now interpreted as the deuteron mass $M_d \approx 2M$. For inelastic scattering from the deuteron the very large proportion of the cross section comes from the kinematic region corresponding to one of the nucleons in the deuteron serving as a spectator and the other as the target—i.e., for $w_d \equiv 2M_d\nu/Q^2 > 2$. When one probes into the region $1 < w_d < 2$ which is also kinematically allowed, one is simultaneously probing into very large momentum components of the deuteron wave function. To see this most directly, we compute the invariant mass of the intermediate proton formed from the bound deuteron and moving in the infinite-momentum center-of-mass frame for the deuteron plus incident electron as used in (7). The result by a straightforward calculation with the kinematics shown in Fig. 11 is

$$\mathfrak{M}^2 - M^2 = -M^2\left(\frac{(w_d\eta'-2)^2}{w_d\eta'(w_d\eta'-1)}\right) + \frac{4M\epsilon}{\eta' w_d},$$

where $0 < \eta' < 1$ is the fraction of longitudinal momentum of the intermediate proton retained on the final proton, and $(1-\eta')$ is the fraction acquired by all the other hadrons produced from the proton. This shows

[10] The data as shown in Fig. 12 suggest some curvature near the threshold and can be fitted approximately by a quadratic curve. These data clearly cannot be used to determine the curvature very accurately, however.

[11] If the baryon is built up of constituents or "partons" of spin 0 and $\frac{1}{2}$ only with minimal coupling to the electromagnetic fields as in our model, there is no possibility for C-violation asymmetries to appear due to the restraints imposed by current conservation alone.

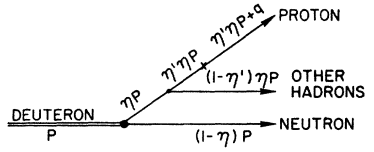

FIG. 11. Diagram for inelastic scattering from the deuteron. We suppress the transverse momenta in writing the labels for the kinematics as illustrated.

that only for $w_d=2/\eta'\geq 2$ are the low momentum components of the deuteron contributing so that the deuteron wave function does not severely damp the amplitudes νW_2 and W_1. In order to continue to the colliding beam region as we did for proton targets, it would be necessary to continue across the boundary from $w_d>1$ to $w_d<1$. However, once w_d decreases below $w_d=2$, we have seen that the inelastic scattering is very severely dampened, and hence we can expect the same very small cross section for deuteron production in e^-e^+ annihilation processes where $w_d<1$.

IV. DEEP-INELASTIC NEUTRINO SCATTERING

Turning to the deep-inelastic neutrino processes (iii) and (iv), we can borrow heavily from the discussions of inelastic electron scattering in Sec. II. The kinematics are the same and since we work to lowest order in the weak as well as the electromagnetic interactions the transition between the electromagnetic and weak scattering can be described as follows, in terms of the bare currents needed for the parton model as shown in Sec. II[12]:

	Electron scattering	Neutrino scattering
Lepton current	$\bar{\psi}_l\gamma_\mu\psi_l$	$\bar{\psi}_l\gamma_\mu(1-\gamma_5)\psi_{\nu_l}$
Coupling	$e^2/q^2=4\pi\alpha/q^2$	$G/\sqrt{2}$
Hadron current	$\bar{\psi}_p\gamma_\mu\psi_p+i\pi^+\overleftrightarrow{\partial_\mu}\pi^-$	$\bar{\psi}_n\gamma_\mu(1-\gamma_5)\psi_p$ $+\sqrt{2}i\pi^+\partial_\mu\pi^0$

(31)

An additional factor of 2 appears in the neutrino cross section because the neutrinos are all left-handed and so there is no spin averaging.

As indicated in (5) and (6), a third structure function is introduced by the presence of parity-violating terms in the weak interaction. The formal derivation of the parton model sketched in Sec. II for inelastic electron scattering is only slightly altered by the appearance of the parity-violating term in the Cabibbo current.[13] Thus, we may consider separately the contributions to the structure functions in (5) from the pion current introduced by the conservation of vector current (CVC) into (31) and from the nucleon current.

[12] We neglect strange particles, which means reducing $SU(3)$ to the isotopic spin or $SU(2)$ classification and setting the Cabibbo angle $\theta_c=0$. Refinements to include such effects can be made and are of negligible effect in the present context since $\theta_c=0$.

[13] Since there are now three structure functions in $W_{\mu\nu}'$, we must also compute with one bad component of the current in (5). The fourth paper in this series presents the detailed derivation of the parton model in this case.

In kinematic regions where the pion current contribution is dominant, as we have conjectured below (28) to be the case near $w=1$, $W_3'^\pi=0$ since there is no bare axial pion current in (31). Also $W_1'^\pi=0$ as in the electromagnetic process because the convection current of spinless pions is along P_μ in the infinite-momentum frame, and therefore only W_2' in (5) is nonvanishing. By a simple isotopic consideration,

$$W_2'^\pi(\nu p)+W_2'^\pi(\nu n)=4W_2^\pi(ep); \tag{32}$$

and by (2) and (6),

$$\left.\frac{d^2\sigma(\nu p)+d^2\sigma(\nu n)}{d^2\sigma(ep)}\right|_\pi=\frac{G^2(Q^2)^2}{2\pi^2\alpha^2}=10^{-7}\left(\frac{Q^2}{M^2}\right)^2.$$

The nucleon and antinucleon currents contribute to all three structure functions. The parton model allows us to determine their ratios readily when we recall that in the infinite-momentum frame the final nucleon or antinucleon emerging with four-momentum p_n+q, $(p_n+q)^2=M^2$, absorbs the virtual "intermediate boson" in the last step of the perturbation expansion so that the matrix element is proportional to

$$\begin{aligned}&\bar{u}(p_n+q)\gamma_\mu(1-\gamma_5)u(p_n)\cdots \quad \text{(nucleon)},\\ &\cdots\bar{v}(p_n)\gamma_\mu(1-\gamma_5)v(p_n+q) \quad \text{(antinucleon)},\end{aligned} \tag{33}$$

where dots denote all that has happened before. This means a contribution to $W_{\mu\nu}'$ of form, after spin sums,

$$\begin{aligned}W_{\mu\nu}'\sim\cdots&(\gamma p_n+M)\gamma_\mu(1\pm\gamma_5)\\ &\times(\gamma p_n+\gamma q+M)\gamma_\nu(1\pm\gamma_5)(\gamma p_n+M)\cdots,\end{aligned} \tag{34}$$

where the $(1-\gamma_5)$ is for the current landing on a nucleon line, and the $(1+\gamma_5)$ by charge conjugation is for the current landing on an antinucleon line. We can further reduce this expression by anticipating the contraction of $W_{\mu\nu}'$ with the lepton spinors as well as the fact that after integration over all internal loops in $W_{\mu\nu}'$, there remain only the two momenta q and P out of which to construct $W_{\mu\nu}'$. Furthermore, the mass shell condition $(p_n+q)^2=M^2$ and the fundamental assumption in our derivation of the parton model that the transverse momenta are bounded so that $\mathbf{p}_n$ and $\mathbf{P}$ are parallel in the infinite-momentum frame combine to fix the ratio $|\mathbf{p}_n|/|\mathbf{P}|=1/w$. This is seen to follow from (13). Therefore, one can write

$$\begin{aligned}W_{\mu\nu}'\sim\cdots&[8P_\mu P_\nu(1/w^2)-2g_{\mu\nu}Q^2\pm 4i\epsilon_{\mu\nu\sigma\tau}P^\sigma q^\tau(1/w)]\\ &\times(\gamma p_n+M)\cdots\end{aligned} \tag{35}$$

and simply read off the ratio of structure functions by comparison with (5):

$$W_1'^N/\nu W_2'^N=w/2M, \quad \nu W_3'^N/\nu W_2'^N=\pm w. \tag{36}$$

Again the + and − signs apply for the current landing on a nucleon and antinucleon line, respectively. Collecting, we can write as a general formula for deep-inelastic

neutrino scattering,

$$\frac{d^2\sigma^{\nu p}}{d\epsilon' d\cos\theta}=\frac{G^2}{\pi}\epsilon'\left(\frac{\epsilon'}{\nu}\right)\Big\{(\nu W_2')^N\Big[\cos^2(\tfrac{1}{2}\theta)+\left(\frac{w\nu}{M}+\frac{2\epsilon-\nu}{M}w\right)\times\sin^2(\tfrac{1}{2}\theta)\Big]+(\nu W_2')^\pi[\cos^2(\tfrac{1}{2}\theta)]+(\nu W_2')^{\bar N}\times\Big[\cos^2(\tfrac{1}{2}\theta)+\left(\frac{w\nu}{M}-\frac{2\epsilon-\nu}{M}w\right)\sin^2(\tfrac{1}{2}\theta)\Big]\Big\}. \quad (37)$$

Insert the following variables:

$$Q^2=4\epsilon^2(1-y)\sin^2(\tfrac{1}{2}\theta), \quad y=\nu/\epsilon$$
$$d\epsilon' d\cos\theta=(My/1-y)dyd(1/w).$$

Taking advantage of the fact that $\nu W_2=F(w)$ is a function of w alone in the Bjorken limit to perform the integral over the inelasticity $\int_0^1 dy$, we find

$$\frac{d\sigma^{\nu p}}{d(1/w)}=\int_0^1 dy\frac{G^2}{\pi}(M\epsilon)[(\nu W_2')^N+(\nu W_2')^\pi(1-y)+(\nu W_2')^{\bar N}(1-y)^2]$$
$$=(G^2/\pi)(M\epsilon)[(\nu W_2')^N+\tfrac{1}{2}(\nu W_2')^\pi+\tfrac{1}{3}(\nu W_2')^{\bar N}]. \quad (38)$$

As is readily verified by comparing the lepton traces, the cross sections for antineutrino processes differ from the above only by the interchange in the numerical coefficients 1 and $\frac{1}{3}$, respectively, multiplying the contributions of the nucleon and antinucleon current interactions to the structure functions.

In the field-theory model of Ref. 1, the nucleon current was found to be dominant in the very inelastic region with $w\gg1$—i.e., to leading order in $\ln w>1$ for each order of interaction the current landed on the nucleon line. We find in this region, therefore, that the neutrino cross section is given by

$$d\sigma^{\nu p}=(G^2/\pi)(M\epsilon)d(1/w)(\nu W_2')^N. \quad (39)$$

In this kinematic region, the dominant family of graphs according to our model is as illustrated in Fig. 9, and we can use simple charge symmetry to identify the neutrino reactions (via a W^+) on protons with antineutrinos (via a W^-) on neutrons, and vice versa. In particular, because of the factors from the lepton traces,[14]

$$d\sigma^{\nu p}=3d\sigma^{\bar\nu n},$$
$$d\sigma^{\nu n}=3d\sigma^{\bar\nu p}, \quad (40)$$

and

$$d\sigma^{\nu p}+d\sigma^{\nu n}=3(d\sigma^{\bar\nu p}+d\sigma^{\bar\nu n}) \quad \text{for} \quad w\gg1.$$

Another consequence of the ladder graphs is that the cross sections on neutrons and protons are equal as shown for inelastic electron scattering in Ref. 1—i.e., for $w\gg1$,

$$d\sigma^{\nu p}=d\sigma^{\nu n}=3d\sigma^{\bar\nu p}=3d\sigma^{\bar\nu n}. \quad (41)$$

Equation (40) or (41) tells us that the ratio of the limiting cross sections for large w is 3 to 1 for neutrinos relative to antineutrinos.

This ratio of 3 to 1 in the large-w very inelastic region is the most striking prediction from our field-theoretic basis for deriving the Bjorken limit. It presents a clear experimental challenge. For inelastic electron scattering Harari[15] has discussed the interpretation of the inelastic structure functions in terms of the contribution of the Pomeranchukon to the forward virtual Compton cross section. Adapting this interpretation to the neutrino process, the fact that the ν to $\bar\nu$ ratio differs from unity tells us that in our model the weak coupling of the Pomeranchukon depends on helicity—i.e., its vector and axial-vector contributions are in phase and interfere. In fact, it can be readily verified that only left-handed currents couple to the hadron amplitude (35) when viewed in the proton rest system. To understand this we recall the basic assumption of our model that all momenta and in particular the internal momenta of the nucleon's structure are small in comparison with the asymptotically large Q^2 and $|\mathbf{q}|=(\nu^2+Q^2)^{1/2}\approx\nu$ delivered by the current from the lepton line. Therefore in the Bjorken limit the current as viewed from the laboratory frame enters an assemblage of "slow" constituents of the nucleon, and the one on which it lands recoils ultrarelativistically with $\mathbf{q}$, leaving the others behind. According to our model, as illustrated in Fig. 9 for $w\gg1$, the constituent on which the bare current lands is a nucleon, and by (31) that nucleon emerges with left-handed helicity—a state which could not be created by a right-handed polarized current component. Thus right-handed currents are absent from our model when the interaction is on the nucleon line.

Finally we can use our model to compute the ratio of neutrino to electron scattering as a check against recent data reported at the 1969 CERN Weak Interaction conference.[16] It is clear from (34) and (35) that the factors $(1-\gamma_5)$ in the current just lead to an additional factor of 2 in W_2' arising from the fact that $(1-\gamma_5)^2=2(1-\gamma_5)$. Furthermore, there are no isotopic factors since, by (41), the neutron and proton cross sections are the same for neutrino as for electromagnetic processes in our model for large w. Therefore we have

$$(\nu W_2')^N=2(\nu W_2). \quad (42)$$

Since the observed behavior of νW_2 in the electron scattering experiments as shown in Fig. 12 weights the large-w region relatively heavily and falls off for $w\lesssim3$, we can make an approximate prediction for the neutrino cross section in (39) by applying our result that the

[14] Relation (40) was independently noticed by J. D. Bjorken (private communication).

[15] H. Harari, Phys. Rev. Letters 22, 1078 (1969).

[16] D. H. Perkins, in Proceedings of CERN Topical Conference on Weak Interactions, 1969, pp. 1–42 (unpublished).

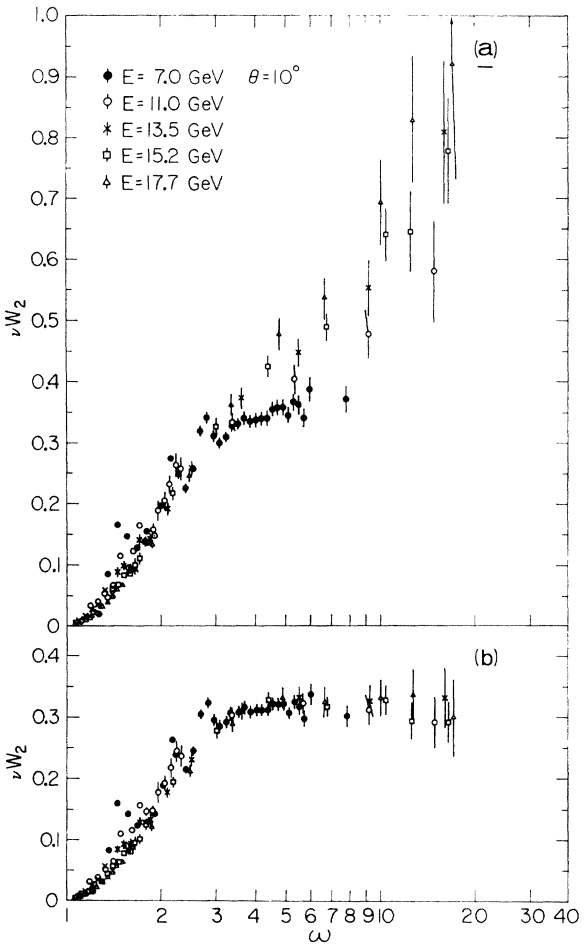

FIG. 12. νW_2 versus $\omega=2M\nu/q^2$ is shown for various assumptions about $R=\sigma_S/\sigma_T$: (a) 10° data for $R=\infty$; (b) 10° data for $R=0$.

nucleon current dominantes throughout the entire w interval in (39). Then, as observed by Bjorken and Paschos,[3] experimentally

$$\int_0^1 d(1/w)(\nu W_2)=0.16$$

and by (39), (41), and (42)

$$\sigma^{\nu p}=\sigma^{\nu n}\approx(2G^2/\pi)(M\epsilon)(0.16)$$
$$=(4\times10^{-39}\ \text{cm}^2)\epsilon\quad(\epsilon\text{ in GeV}).\qquad(43)$$

This agrees within a factor of 2 with the CERN bubble-chamber data[16] in the energy ranges up to $\epsilon_{\max}\approx10$ GeV. We also notice that if the contributions to $(\nu W_2')$ were attributed to the pion current, then by (32) and (38) the same result as (43) would be obtained for the average nucleon cross section $\frac{1}{2}(\sigma^{\nu p}+\sigma^{\nu n})$; but in this case the ν and $\bar{\nu}$ cross sections would be equal instead of in the ratio of 3:1 for large w.

V. SUMMARY AND CONCLUSION

We have constructed a formalism for deriving the inelastic structure functions in the Bjorken limit—i.e., the "parton" model—from canonical field theory. To accomplish this derivation it was necessary to *assume* that there exists an asymptotic region in which the momentum and energy transfers to the hadrons can be made greater than the transverse momenta of their virtual constituents, or "partons" in the infinite-momentum frame.

In addition to deriving the inelastic scattering structure functions, we have accomplished the crossing to the annihilation channel and established the parton model for deep inelastic electron-positron annihilation. We found as an important consequence of this derivation that the deep-inelastic annihilation processes have very large cross sections and have the same energy dependence, at fixed $w\equiv2M\nu/q^2$, as do the point lepton cross sections. Moreover, these cross sections are orders of magnitude larger than the two-body process $e^-+e^+\rightarrow p+\bar{p}$. If verified this result has important experimental implications since it suggests that there is a lot of interesting and observable physics to be done with colliding rings. Some general implications for experiments which detect single hadrons in the final states (sum rules) were also discussed and specific quantitative predictions were presented on the basis of our pion-nucleon field-theory model.

Finally we studied the deep-inelastic neutrino cross sections, deriving the parton model in the presence of the additional parity-violating term in the $(V-A)$ interaction. We computed the ratio of neutrino and antineutrino cross sections to inelastic electron scattering and compared the predictions with data.

To conclude, we raise the two central questions *not* answered by this work:

(1) Where does the transverse-momentum cutoff come from?

(2) How can one understand the rapid decrease of the elastic electromagnetic form factors that fall off as $1/q^4$ with increasing q^2 on the basis of our canonical field theory of the inelastic structure functions?

(1) We *assumed* that we could casually let q^2 and $M\nu$ be asymptotically larger than all masses or internal loop momenta in deriving the parton model. However, when we actually calculate specific terms to a given order in the strong coupling we find [see Eqs. (25) and (29), for example] that formally diverging expressions result if we take the q^2 and $M\nu\rightarrow\infty$ limit in the integrand. This reflects the property of a renormalizable field theory, as opposed to a super-renormalizable one with trilinear coupling of spin-0 particles, that it has no extra momentum powers to spare in the integrals over loops and bubbles in Feynman graphs. This also is reflected in the failure to find the Bjorken limit in perturbation calculations as has been observed by many who have come up with extra factors in $\ln q^2$

in specific calculations.[17] It is our general view that if we are to look for clues to understanding the behavior of hadrons in canonical field theory, we must choose a starting point for an iteration procedure that has some features not too grossly in conflict with the phononena in the real world. Presumably an exact solution of field theory would reproduce the observed rapid falloff both of the elastic electromagnetic form factors of the proton and of the transverse momentum transfer distributions in high-energy inelastic hadron interactions. Yet these behaviors cannot be deduced by iterative calculations starting with local canonical field theory. In our analysis what we have done is to insert this constraint suppressing large momentum transfers by hand. We presume—and it is no more than a statement of faith—that were the exact solutions within our ability to construct, we would observe them to exhibit this behavior. Having assumed such a cutoff, we have succeeded in developing a formalism that converges in the Bjorken limit, which yields the parton model behavior, and which, by explicit calculation, obeys the strictures of crossing symmetry. We used this formalism to make definite predictions for experimental testing of the relation of deep inelastic electron-positron annihilation and neutrino-scattering processes to the inelastic electron scattering. Moreover, detailed predictions on the structure of the inelastic scattering cross sections are also made.

(2) Once we adopt the approach of field theory with a cutoff we must then interpret the vanishing of the elastic form factors as $|q^2| \to \infty$ by setting the vertex and wave-function renormalization constants to zero. To show this we undress the current in the elastic matrix element, using (8), and write

$$\langle P'|J_\mu|P\rangle = \langle UP'|j_\mu|UP\rangle .$$

Since the bare current j_μ is a one-body operator, it can connect only the projection of $|UP\rangle$ onto a one-particle state with momentum $\mathbf{P}$ with the similar projection of $|UP'\rangle$ with momentum $\mathbf{P}'=\mathbf{P}+\mathbf{q}$. There is no overlap of two or more particle amplitudes in $|UP\rangle$ and $|UP'\rangle$ since, with our cutoff model, all the constituents are focused along the two different momentum vectors $\mathbf{P}$ and $\mathbf{P}'$, respectively, with vanishing overlap for large $\mathbf{q}$. With the familiar identification of $\sqrt{Z_2}$ as the wave-function renormalization, we write according to old-fashioned perturbation theory

$$|UP\rangle = (\sqrt{Z_2})\{|P\rangle + 0(g)|\pi_{\mathbf{k}}, N_{\mathbf{P}-\mathbf{k}}\rangle + \cdots\} \quad (44)$$

and thus

$$\langle P'|J_\mu|P\rangle = Z_2\{\langle P'|j_\mu|P\rangle + 0(g^2)\langle N_{\mathbf{P}'-\mathbf{k}'}\pi_{\mathbf{k}'}|j_\mu|N_{\mathbf{P}-\mathbf{k}}\pi_{\mathbf{k}}\rangle\cdots\}. \quad (45)$$

For large q^2 this becomes

$$\langle P'|J_\mu|P\rangle \to Z_2\langle P'|j_\mu|P\rangle + O(1/q^2),$$

indicating that Z_2, the coefficient of the bare matrix element, must vanish if this theory is to lead to a vanishing of the form factor at large q.

When we turn now to the calculation of the inelastic structure functions we are interested in the diagonal matrix element of a bilinear form in the current operators. Once again the U transformation introduces an overall multiplicative factor of $\sqrt{Z_2}$ as in (44) when we work in terms of the bare point current operators. If $Z_2=0$, then either the structure functions also vanish or the sum of contributions of all the multiparticle terms in (44) add up to cancel the Z_2 just as they do in the normalization integral

$$\langle UP'|UP\rangle = \delta^3(\mathbf{P}'-\mathbf{P}) = \delta^3(\mathbf{P}'-\mathbf{P})Z_2[1+O(g^2)\cdots].$$

We assume this to be the case. Although we cannot verify it by direct calculation, we nevertheless offer two further remarks to indicate that this assumption is not unreasonable provided $Z_2=0$ is a self-consistent dynamical requirement. First, (45) seems to suggest that if $Z_2=0$, the nucleon electromagnetic form factors not only vanish asymptotically for large q^2 but also vanish identically for all values of q^2, since Z_2 appears as an over-all multiplicative factor. This, of course, cannot be true as the charge form factor of the proton has a fixed value unity at $q^2=0$ independent of Z_2. Second, the inequality (14) also implies that νW_2 cannot vanish identically. In fact, the integral as shown has a lower bound unity, independent of the value of Z_2. Thus we conclude that if $Z_2=0$ is a self-consistent dynamical requirement of an exact theory, it in no way contradicts the rapid falloff of the nucleon electromagnetic form factors with large q^2 and the nonvanishing of the structure functions for the inelastic electron-proton scattering in the Bjorken limit.

With reference to the detailed analysis of Ref. 1 for inelastic scattering, we recall that we worked in the asymptotic region of $\ln w \gg 1$ as well as Q^2, $2M\nu \to \infty$ and computed W_1 and νW_2 by summing leading terms in the expansion of $g^2 \ln w$ to all orders. Our working assumption, as discussed there, was that the sum of leading terms order by order converged to the correct sum for large w. Thus we summed the top row in the series

$$\frac{1}{w}\Big[1+\xi\ln w+\frac{\xi^2}{2!}\ln^2 w+\frac{\xi^3}{3!}\ln^3 w+\cdots + O(\xi)+O(\xi^2\ln w)+O(\xi^3\ln^2 w)+\cdots + O(\xi^2)+O(\xi^3\ln w)+\cdots + O(\xi^3)+\cdots\Big]. \quad (46)$$

What our conjecture amounts to is this: If we add up the powers in the coupling constant expansion by summing along the diagonal in (46), we will actually cancel the renormalization constant Z_2.

[17] Y. S. Tsai (private communication); S. L. Adler and Wu-Ki Tung, Phys. Rev. Letters **22**, 978 (1969); R. Jackiw and G. Preparata, *ibid.* **22**, 975 (1969).